Turkish Journal of Chemistry

http://journals.tubitak.gov.tr/chem/

Research Article

Turk J Chem
(2019) 43: 1552 – 1569

doi:10.3906/kim-1907-71

Design, synthesis, and antitumor evaluation of novel methylene moiety-tethered tetrahydroquinoline derivatives

Essam Hamied Ahmed HANASHALSHAHABY[1], **Canan ÜNALEROĞLU**[1], **Ayşe AK CAN**[2,3], **Alp ÖZGÜN**[2], **Bora GARİPCAN**[2,*]

[1]Department of Chemistry, Faculty of Science, Hacettepe University, Beytepe Campus, Ankara, Turkey
[2]Institute of Biomedical Engineering, Boğaziçi University, Kandilli Campus, Çengelköy, İstanbul, Turkey
[3]Medical Imaging Techniques Program, Vocational School of Health Services, Kocaeli University, Kocaeli, Turkey

Received: 29.07.2019 • **Accepted/Published Online:** 01.10.2019 • **Final Version:** 09.12.2019

Abstract: Novel methylene-tethered tetrahydroquinolines (THQs) and cyclopenta[*b*]pyridines were synthesized by one-pot multicomponent reactions of Mannich bases, enolizable ketones, and NH_4OAc in water by an environmentally friendly K-10 montmorillonite clay-catalyzed reaction. The cytotoxic activities of 1-(2-methyl-8-methylene-5,6,7,8-tetrahydroquinolin-3-yl)ethanone (**9a**), ethyl 2-methyl-8-methylene-5,6,7,8-tetrahydroquinoline-3 carboxylate (**9b**), and 1-(2-methyl-7-methylene-6,7-dihydro-5*H*-cyclopenta[*b*]pyridin-3-yl)ethanone (**11a**) were tested against rat glioblastoma (C6), human breast cancer (MCF-7), prostate cancer (PC3), neuroblastoma (SH-SY5Y), and mouse fibroblast (L929) cell lines in a concentration-dependent (50–300 µM) and time-dependent (24–72 h) manner and expressed as IC_{50} values. The results showed that compound **9a** induced the lowest IC_{50} values in all cell lines ranging from 111 ±1.1 µM to 128 ±1.3 µM when compared to **9b** and **11a** after 72 h. As an evaluation of antibacterial properties, a swarming motility assay was performed with the *Pseudomonas aeruginosa* PA01 strain and compound **9a** showed higher inhibition of swarming motility.

Key words: Tetrahydroquinolines, antitumor activity, Mannich base, green synthesis, multicomponent reaction, heteroaromatics

1. Introduction

Cancer is the second main cause of death worldwide [1]. A large number of studies have been devoted to exploring new biologically active compounds as antitumor therapeutic agents to be used in chemotherapeutic drug systems [2,3]. In this regard, the synthesis of new organic molecules for bioactivity evaluation or modification studies on molecules creates a wide working area for synthetic chemists. In recent years, tetrahydroquinolines (THQs) have been considered to be one of the pharmaceutical agents that have the greatest interest in the chemistry of quinolines due to their broad biological and pharmacological activities [4–7]. The most potent effects among a variety of pharmacological activities are exhibited by 1,2,3,4-THQs [8–12], such as glucocorticoid receptor agonists [13], antagonists of vasopressin V_2 receptor [14], and antitumor agents targeting the colchicine site on tubulin [15]. A second type of THQ with the 5,6,7,8-THQ structure has appeared in some reports in which their potential biopharmaceutical effects were evaluated [16–18]. Recently, 5,6,7,8-THQ derivatives have been presented to act as anti-HIV-1 agents [19], anticancer agents [20], and antagonists against

*Correspondence: bora.garipcan@boun.edu.tr

metabotropic glutamate receptors (mGluRs) **1** (Figure 1), which play a crucial role in the prevention and control of acute neurological disorders [21]. A recently published study illustrated that a wide variety of 5,6,7,8-THQ derivatives have exhibited remarkable cytotoxic activity against human colon carcinoma HT29, hepatocellular carcinoma HepG2, and Caucasian breast adenocarcinoma MCF-7 cells lines [22]. Furthermore, antiulcer and/or antisecretory activities of a number of 5,6,7,8-THQ-8-nitriles, thioamides, and thiocarbamoylamines have been reported [23,24]. Arylidine-tethered THQs **2** have found uses as inhibitors of both the synthesis of leukotrienes and the action of lipoxygenase in mammalian metabolism (Figure 1) [25,26].

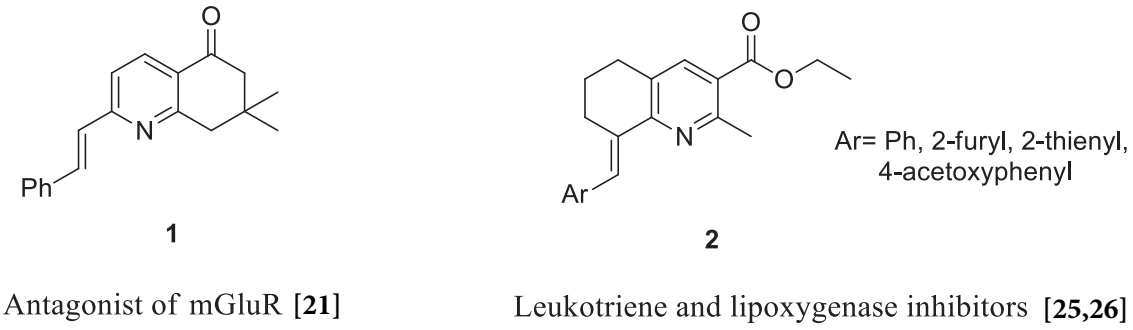

Figure 1. Biologically active 5,6,7,8-THQ derivatives.

As noted in the aforementioned reports, various pharmacological activities of 8-substituted-5,6,7,8-THQ derivatives play a key role in medicinal chemistry. Therefore, synthesis of new methylene-tethered 5,6,7,8-THQs is important for investigating their medicinal applications. The authors recently reported a new synthetic approach for the synthesis of 2,3,6-trisubstituted pyridines and 5,6,7,8-THQs [27] and used them in this study for the synthesis of new methylene-tethered THQs and cyclopenta[*b*]pyridines. The retrosynthetic strategy given in Figure 2 illustrates the synthesis of the target molecules. In this strategy, target molecules **6** were obtained efficiently from K-10 montmorillonite clay-catalyzed multicomponent reactions (MCRs) of the Mannich base enone precursors of **4** and **5**, enolizable ketones **3**, and NH_4OAc with an environmentally friendly reaction protocol. As part of our ongoing work on quinoline chemistry, we herein report a new approach for the synthesis of new methylene-tethered THQs and cyclopenta[*b*]pyridines to explore their cytotoxic effects on rat glioblastoma (C6), human breast cancer (MCF-7), prostate cancer (PC3), neuroblastoma (SH-SY5Y), and mouse fibroblast (L929) cell lines.

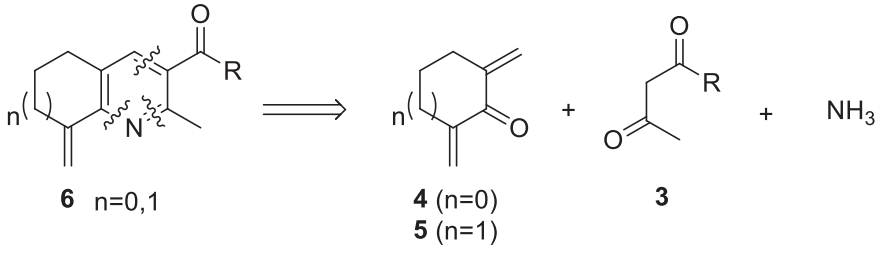

Figure 2. Retrosynthetic strategy for the synthesis of 5,6,7,8-THQs.

2. Results and discussion

2.1. Chemistry

1-(2-Methyl-8-methylene-5,6,7,8-tetrahydroquinolin-3-yl)ethanone (**9a**), ethyl 2-methyl-8-methylene-5,6,7,8-tetrahydroquinoline-3-carboxylate (**9b**), 1-(2-methyl-7-methylene-6,7-dihydro-5*H*-cyclopenta[*b*]pyridin-3-yl) ethanone (**11a**), and ethyl 2-methyl-7-methylene-6,7-dihydro-5*H*-cyclopenta[*b*]pyridine-3-carboxylate (**11b**) were synthesized according to the synthetic plan outlined in Figure 3. In this approach, Mannich bases **7** and **10** were used as 2,6-dimethylenecyclohexanone (**5**) and 2,5-dimethylenecyclopentanone (**4**) precursors, respectively. It is commonly known that vinyl ketones are usually unstable and expensive materials [28,29]. Therefore, key components 2,6-dimethylenecyclohexanone and 2,5-dimethylenecyclopentanone were obtained in situ from Mannich bases **7** and **10**, which were easily prepared from commercially available starting materials according to the methods reported in the literature [30].

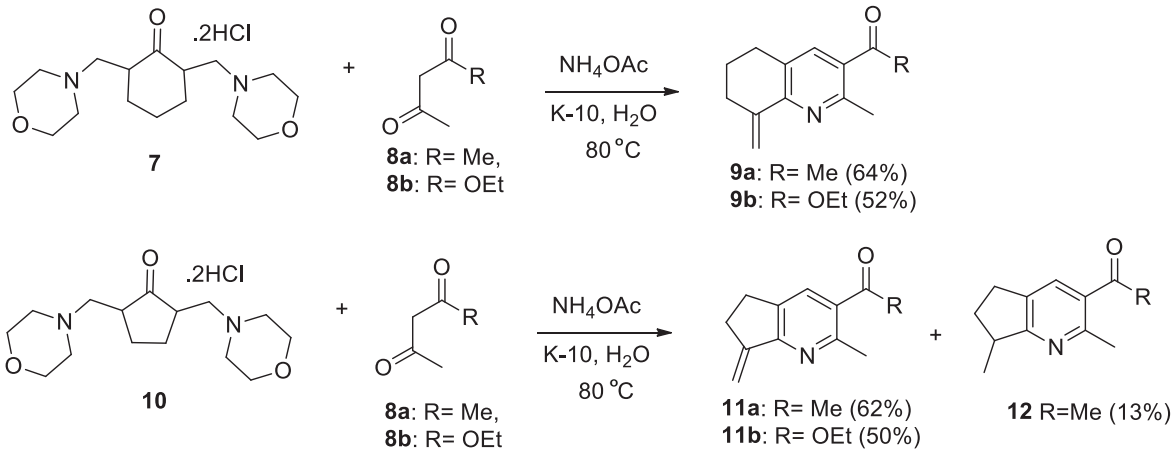

Figure 3. Synthesis of 9a, 9b,11a, and 11b.

First, we considered the domino reaction of Mannich base **7**, enolizable ketone **8a**, and ammonia to obtain 1-(2-methyl-8-methylene-5,6,7,8-tetrahydroquinolin-3-yl)ethanone (**9a**). The synthesis of **9a** was easily achieved starting from commercially available ketone **8a**, Mannich base **7**, and ammonia in the presence of the environmentally friendly K-10 montmorillonite clay catalyst in water. The reaction produced desired product **9a** with 64% yield. Ethyl 2-methyl-8-methylene-5,6,7,8-tetrahydroquinoline-3-carboxylate (**9b**) was synthesized from the reaction of Mannich base **7**, β-keto ester **8b**, and ammonium acetate with 52% yield. The same synthetic approach was used for the synthesis of **11a** and **11b**. One-pot MCRs of Mannich base **10**, **8a**, **8b**, and NH_4OAc gave corresponding products **11a** (62%) and **11b** (50%), respectively. When pentane-2,4-dione (**8a**) was used as an enolizable ketone, a second product (**12**) was isolated with 13% yield. A similar result was observed for the formation of **9a**; however, it formed in trace amounts. All products were purified by flash column chromatography and characterized by ^{1}H NMR, ^{13}C NMR, and HRMS analyses.

2.2. Biology

In vitro cytotoxicity of synthesized compounds **9a**, **9b**, and **11a** was investigated by using rat glioblastoma (C6), human breast cancer (MCF-7), prostate cancer (PC3), neuroblastoma (SH-SY5Y), and mouse fibroblast

(L929) cell lines under the same conditions using the MTT assay [31]. Due to its low solubility, compound **11b** could not be used in the cytotoxicity experiments. The cytotoxic activities of compounds **9a**, **9b**, and **11a** were tested in a concentration-dependent (50–300 µM) and time-dependent (24–72 h) manner and expressed as IC_{50} values (Table 1). The results showed that compound **9a** has the lowest IC_{50} values for all cell lines, ranging from 111 ±1.1 µM to 128 ±1.3 µM (Table 1), when compared to **9b** and **11a** after 72 h. The IC_{50} values did not vary significantly depending on cell line for compound **9a**. At the lower dose (50 µM) compound **9a** showed little or no cytotoxicity after 24 h for all cell lines. However, after 72 h, compound **9a** decreased the viability of all cell lines except SH-SY5Y. At a higher dose (300 µM), SH-SY5Y cells showed a rapid cytotoxic response to compound **9a** when compared to other cell lines**.** After 72 h, compound **9a** at 300 µM concentration significantly decreased the viability of all cell lines (Figure 4; Table 2).

At the lower dose (50 µM) compound **9b** showed little or no cytotoxicity after 24 h for all cell lines. However, after 72 h, compound **9b** decreased the viability of all cell lines except SH-SY5Y, similar to compound **9a**. At a higher dose (300 µM), C6 cells showed a rapid cytotoxic response to compound **9b** when compared to other cell lines**.** After 72 h, compound **9b** at 300 µM concentration significantly decreased the viability of all cell lines (Figure 4; Table 2). At the lower dose (50 µM) compound **11a** showed little or no cytotoxicity after 24 h for all cell lines. However, after 72 h, compound **11a** decreased the viability of all cell lines except SH-SY5Y, whose viability even increased, albeit nonsignificantly. At a higher dose (300 µM) SH-SY5Y cells showed a rapid cytotoxic response to compound **11a** when compared to other cell lines. After 72 h, compound **11a** at 300 µM concentration significantly decreased the viability of all cell lines (Figure 4; Table 2).

Table 1. In vitro toxicity screening of synthesized compounds **9a**, **9b**, and **11a** against four cancer cell lines and one normal cell line (given in IC_{50} values; µM ±SD).

IC_{50} values of the compounds (µM)				
Cell lines		**9a**	**9b**	**11a**
C6	24 h	192 ±2.1	245 ±2.7	278 ±3.1
	48 h	122 ±1.2	178 ±1.9	177 ±1.9
	72 h	115 ±1.1	169 ±1.8	164 ±1.7
MCF-7	24 h	375 ±4.2	590 ±6.7	363 ±4.1
	48 h	183 ±1.9	330 ±3.7	206 ±2.2
	72 h	117 ±1.2	187 ±2.0	152 ±1.6
PC3	24 h	280 ±3.1	434 ±4.9	351 ±3.9
	48 h	146 ±1.5	237 ±2.6	190 ±2.0
	72 h	116 ±1.2	147 ±1.5	145 ±1.5
SH-SY5Y	24 h	173 ±1.8	478 ±5.4	219 ±2.4
	48 h	136 ±1.4	160 ±1.7	176 ±1.8
	72 h	128 ±1.3	144 ±1.5	157 ±1.6
L929	24 h	295 ±3.3	303 ±3.4	345 ±3.9
	48 h	140 ±1.4	143 ±1.5	212 ±2.3
	72 h	111 ±1.1	135 ±1.4	127 ±1.3

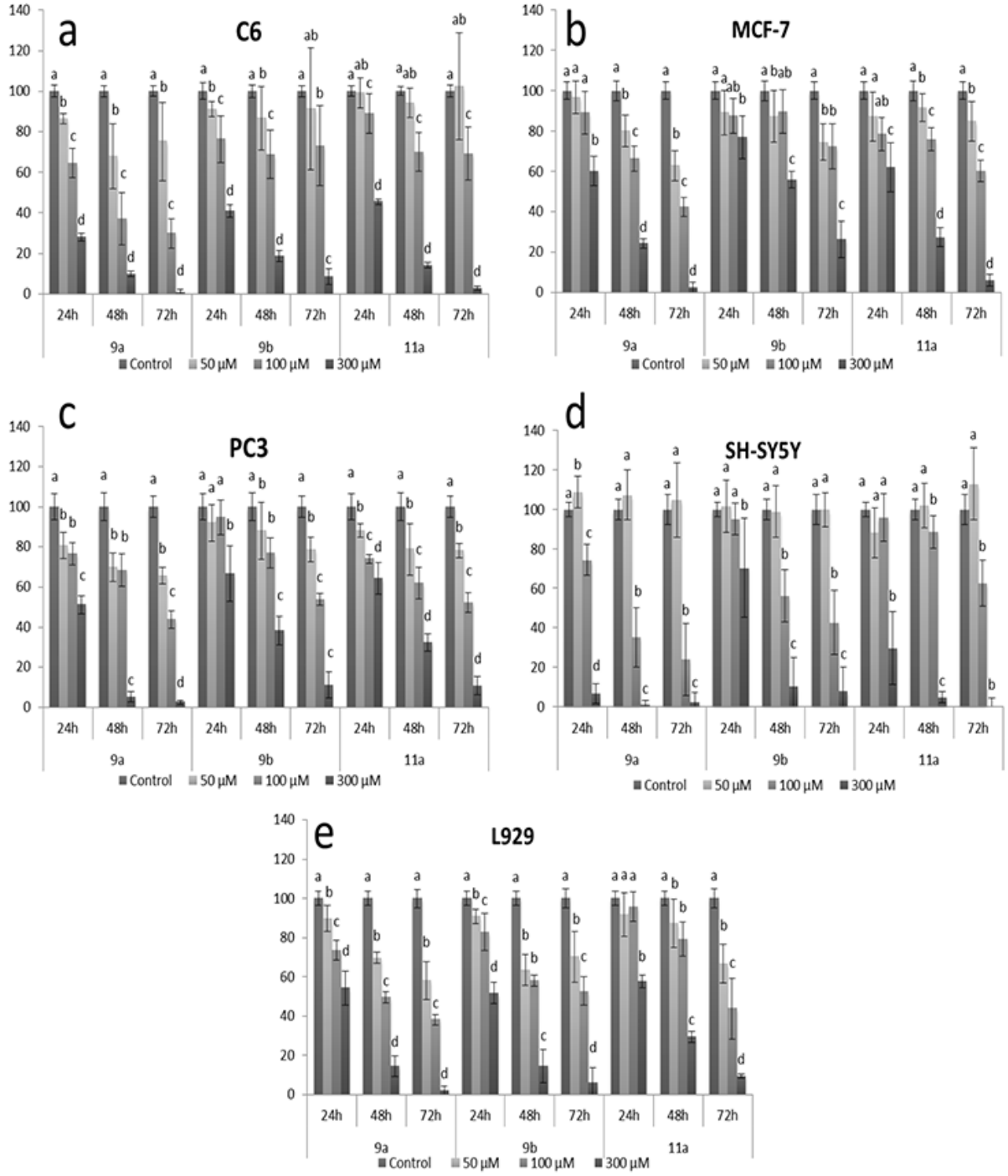

Figure 4. Cell viabilities (%) for **9a**, **9b**, and **11a** at 24, 48, and 72 h: a) rat glioblastoma (C6), b) human breast cancer (MCF-7), c) prostate cancer (PC3), d) neuroblastoma (SH-SY5Y), and e) mouse fibroblast (L929) ($P < 0.05$).

Table 2. Cell viabilities (%) for compounds **9a**, **9b**, and **11a** at 24, 48, and 72 h (P <0.05); values with different letters (a, b, c, d) are significantly different at the 0.05 level.

	9a			**9b**			**11a**			
	Control	50 µM	100 µM	300 µM	50 µM	100 µM	300 µM	50 µM	100 µM	300 µM
C6 Rat glioblastoma										
24 h	100.00 ±2.97^{a}	86.45 ±2.72^{b}	64.66 ±7.13^{c}	28.15 ±1.87^{d}	91.08 ±3.66^{b}	76.42 ±11.49^{c}	40.96 ±3.30^{d}	99.13 ±7.54^{a}	89.10 ±9.82^{b}	45.57 ±1.40^{c}
48 h	100.00 ±2.82^{a}	67.90 ±15.99^{b}	37.13 ±12.88^{c}	9.96 ±1.40^{d}	86.68 ±15.75^{b}	68.86 ±12.04^{c}	18.61 ±2.67^{d}	94.26 ±7.06^{a}	70.03 ±9.49^{b}	14.28 ±1.28^{c}
72 h	100.00 ±2.50^{a}	75.25 ±19.30^{b}	29.95 ±7.18^{c}	0.96 ±1.44^{d}	91.32 ±30.16^{ab}	73.12 ±19.66^{b}	8.60 ±3.90^{c}	102.49 ±26.26^{a}	69.22 ±12.97^{b}	2.87 ±1.12^{c}
MCF-7 Breast cancer										
24 h	100.00 ±4.33^{a}	96.87 ±8.07^{a}	89.12 ±10.50^{a}	60.18 ±7.17^{b}	89.16 ±10.87^{a}	87.48 ±8.66^{ab}	76.94 ±10.54^{c}	87.27 ±12.18^{ab}	78.45 ±8.21^{b}	62.04 ±12.12^{c}
48 h	100.00 ±4.82^{a}	80.02 ±7.83^{b}	66.39 ±6.18^{c}	24.26 ±2.28^{d}	87.39 ±12.83^{b}	89.51 ±10.80^{ab}	55.90 ±4.09^{c}	91.70 ±7.01^{b}	75.88 ±5.71^{c}	27.30 ±4.73^{d}
72 h	100.00 ±4.37^{a}	62.71 ±7.52^{b}	42.31 ±4.70^{c}	2.38 ±2.83^{d}	74.47 ±9.06^{b}	72.38 ±11.07^{b}	26.27 ±9.02^{c}	84.73 ±9.92^{b}	60.33 ±5.31^{c}	6.03 ±2.92^{d}
PC3 Prostate cancer										
24 h	100.00 ±6.66^{a}	80.68 ±6.52^{b}	76.43 ±5.54^{b}	51.10 ±4.53^{c}	91.91 ±9.23^{a}	94.56 ±8.67^{a}	66.77 ±13.92^{b}	88.06 ±3.41^{b}	74.04 ±2.12^{c}	64.26 ±7.95^{d}
48 h	100.00 ±7.00^{a}	69.79 ±7.00^{b}	68.47 ±8.21^{b}	5.14 ±2.56^{c}	87.99 ±14.16^{b}	77.03 ±7.45^{b}	38.30 ±7.19^{c}	78.80 ±12.93^{b}	61.78 ±7.89^{c}	32.23 ±4.33^{d}
72 h	100.00 ±5.19^{a}	65.67 ±4.28^{b}	43.75 ±4.51^{c}	2.55 ±1.07^{d}	78.73 ±6.08^{b}	53.80 ±2.96^{c}	11.19 ±6.63^{d}	78.07 ±3.59^{b}	52.15 ±5.03^{c}	10.68 ±4.64^{d}
SH-SY5Y Neuroblastoma										
24 h	100.00 ±3.63^{a}	108.74 ±8.12^{b}	74.32 ±7.85^{c}	6.67 ±5.03^{d}	101.68 ±13.22^{a}	95.18 ±7.93^{a}	70.26 ±25.13^{b}	88.12 ±12.82^{a}	95.91 ±11.90^{a}	29.66 ±18.36^{b}
48 h	100.00 ±5.10^{a}	107.38 ±12.80^{a}	35.20 ±15.09^{b}	0.95 ±2.00^{c}	98.92 ±12.94^{a}	56.23 ±13.28^{b}	10.54 ±14.35^{c}	101.97 ±11.36^{a}	88.60 ±8.17^{b}	4.69 ±2.75^{c}
72 h	100.00 ±7.60^{a}	104.90 ±18.86^{a}	23.84 ±18.19^{b}	2.30 ±4.84^{c}	99.78 ±8.68^{a}	42.56 ±16.24^{b}	7.83 ±12.29^{c}	112.99 ±18.36^{a}	62.63 ±11.73^{b}	0.10 ±4.31^{c}
L929 Mouse fibroblast										
24 h	100.00 ±3.60^{a}	89.82 ±6.49^{b}	73.57 ±5.09^{c}	54.36 ±8.69^{d}	90.81 ±3.82^{b}	82.97 ±9.35^{c}	51.84 ±5.59^{d}	91.88 ±11.08^{a}	95.86 ±7.61^{a}	57.65 ±3.21^{b}
48 h	100.00 ±3.70^{a}	69.69 ±2.81^{b}	49.59 ±2.69^{c}	14.56 ±5.18^{d}	63.63 ±7.92^{b}	58.12 ±2.66^{b}	14.64 ±8.52^{c}	87.30 ±12.31^{b}	79.33 ±8.67^{b}	29.43 ±2.80^{c}
72 h	100.00 ±4.69^{a}	58.16 ±9.61^{b}	38.27 ±2.62^{c}	2.22 ±2.39^{d}	70.25 ±12.88^{b}	52.67 ±7.27^{c}	6.28 ±7.40^{d}	66.76 ±9.84^{b}	43.93 ±15.53^{c}	9.53 ±1.03^{d}

Acridine orange (AO) and propidium iodide (PI) are nucleic acid binding dyes that can be used to evaluate cell proliferation and viability. AO is a cell-permeable dye and all stained nucleated cells generate a green fluorescence, whereas PI only enters cells with compromised membranes and therefore stained necrotic nucleated cells generate a red fluorescence [31,32]. In order to confirm the in vitro cytotoxicity results obtained from the MTT assay, AO and PI staining was performed to determine cell viability by using rat glioblastoma (C6), human breast cancer (MCF-7), prostate cancer (PC3), neuroblastoma (SH-SY5Y), and mouse fibroblast (L929) cell lines under the same conditions.

Compounds **9a, 9b**, and **11a** at 50 µM concentration showed little or no cytotoxicity after 24 h for all cell lines. After 72 h, compound **9a** had no significant effect on the viability of all cell lines except PC3. At 300 µM concentration, SH-SY5Y cells showed a rapid cytotoxic response to compound **9a** when compared to other cell lines. After 72 h, compound **9b** showed no or little cytotoxicity to all cell lines except MCF-7, which differs from compound **9a**. SH-SY5Y cells showed a rapid cytotoxic response to compound **9b** when compared to other cell lines, similar to compound **9a**. After 72 h, compound **11a** had no significant effect on the viability of all cell lines except L929. At the higher concentration (300 µM) C6 cells showed a rapid cytotoxic response to compound **11a** when compared to other cell lines. After 72 h, compounds **9a**, **9b**, and **11a** at 300 µM concentration significantly decreased the viability of all cell lines (Figures 5 and 6; Table 3).

Apoptosis is mediated by the cascade of aspartate-specific cysteine proteases or caspases. The CellEvent Caspase-3/7 Green Detection Reagent (Invitrogen) was used to determine viable, apoptotic, and necrotic cells [33]. After activation of caspase-3 or caspase-7 in apoptotic cells, the membrane-permeable substrate was cleaved and was able to bind to DNA, and a green fluorescence signal occurred [34].

Caspase activity was determined to distinguish whether apoptosis or necrosis was responsible for PC3 and L929 cell toxicity of compound **9a** (Table 4; Figure 7) according to the IC_{50} values obtained from the MTT assay. The L929 cell line was chosen as having the lowest IC_{50} value (111 $\pm$1.1 µM), whereas the PC3 cell line was chosen as a model cell line that had similar IC_{50} values with respect to the MCF-7 and C6 cell lines (Table 1). As seen in Table 4, apoptosis increased 2.6-fold and necrotic cells increased 3.9-fold when compound **9a** was administered to prostate cancer cells. In the fibroblast cell line, L929, apoptotic cells increased 12-fold and necrotic cells increased 2-fold when compound **9a** was applied.

Herein, we demonstrated that the new methylene-tethered THQ **9a** has higher toxicity than THQ derivatives **9b** and cyclopenta[*b*]pyridine **11a.** Compounds **9a** and **9b** have the same skeleton except for the functional groups. The results indicated that the presence of the ketone moiety on **9a** enhanced the activity of the molecule towards all cells. The IC_{50} values of our compound (**9a**) are close to those of Gedawy et al., who synthesized THQ derivatives and investigated their in vitro anticancer activity against human colon carcinoma (HCT116) and human breast adenocarcinoma (MCF-7) cell lines. Some of these 2,3,4-trisubstituted-5,6,7,8-THQs have shown potent anticancer activity against both HCT116 (IC_{50} values between 61.71 and 75.09 µM) and MCF-7 (IC_{50} values >100 µM) cell lines [4]. Hatano et al. studied the tumor-specific cytotoxicity and type of cell death with THQ derivatives in human oral squamous cells and carcinoma cell lines and their data were similar to our findings [35].

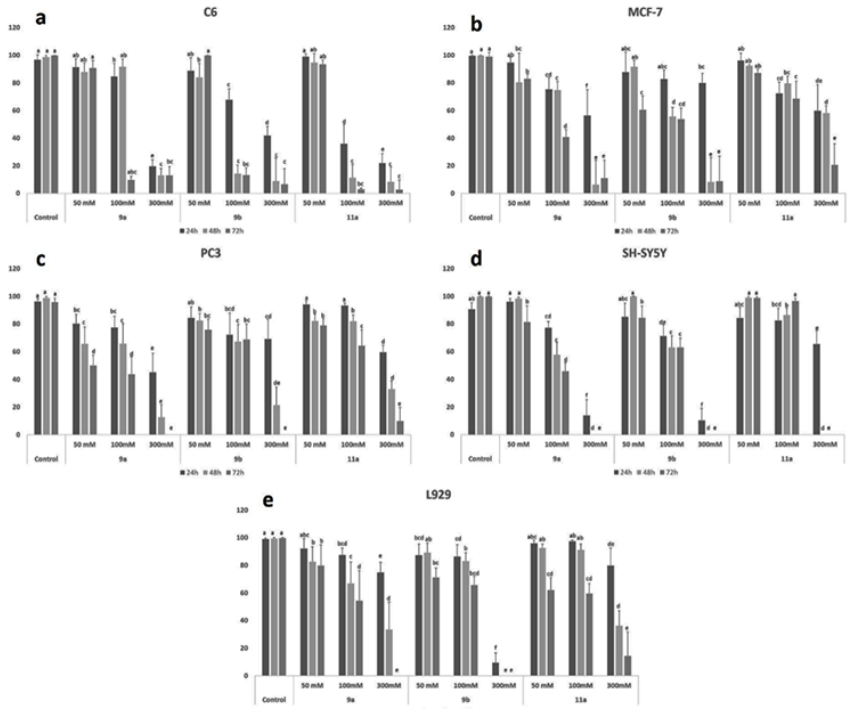

Figure 5. Cell viabilities for **9a**, **9b**, and **11a** at 24, 48, and 72 h: a) rat glioblastoma (C6), b) human breast cancer (MCF-7), prostate cancer (PC3), d) neuroblastoma (SH-SY5Y), and e) mouse fibroblast (L929) as calculated from live and dead stained cells.

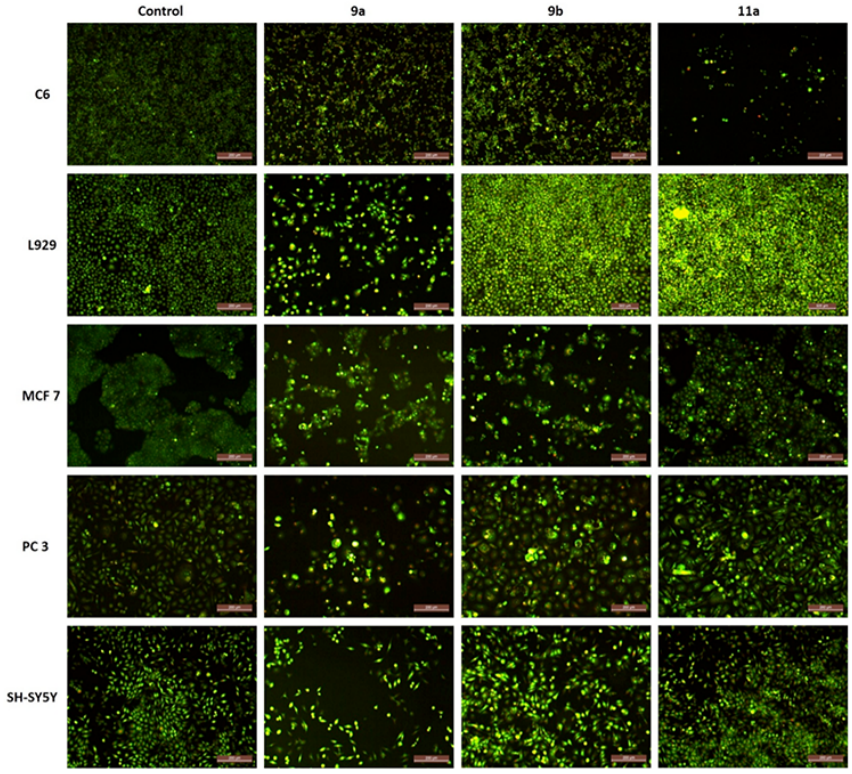

Figure 6. Representative micrographs taken from AO/PI-stained cells treated with 100 µM **9a**, **9b**, and **11a**for 24 h.

Table 3. Cell viability values of compounds **9a**, **9b**, and **11a** at 24, 48, and 72 h as calculated from AO/PI staining ($P < 0.05$).

	9a			**9b**			**11a**			
	Control	50 µM	100 µM	300 µM	50 µM	100 µM	300 µM	50 µM	100 µM	300 µM
C6 Rat glioblastoma										
24 h	96.63 ±3.65^{a}	91.32 ±6.2^{ab}	84.47 ±9.49^{b}	19.51 ±4.86^{e}	88.64 ±9.58^{ab}	67.67 ±7.95^{c}	41.77 ±6.75^{d}	98.92 ±2.13^{a}	35.83 ±13.9^{d}	21.65 ±7.22^{e}
48 h	98.58 ±1.25^{a}	87.74 ±6.45^{ab}	91.6 ±5.67^{ab}	12.83 ±5.16^{c}	83.86 ±10.1^{b}	14.14 ±6.26^{c}	8.68 ±16.89^{c}	94.68 ±6.43^{ab}	11.25 ±9.62^{c}	8.25 ±10.73^{c}
72 h	99.59 ±0.35^{a}	90.75 ±5.35^{a}	9.41 ±2.97^{abc}	12.83 ±6.33^{bc}	99.76 ±0.29^{abc}	13.01 ±5.41^{bc}	6.44 ±11.3^{c}	93.38 ±3.18^{ab}	2.69 ±0.96^{bc}	2.50 ±7.07^{c}
MCF-7 Breast cancer										
24 h	99.34 ±0.63^{a}	94.63 ±3.79^{ab}	75.24 ±8.48^{cd}	56.38 ±18.63^{f}	87.58 ±14.65^{abc}	82.75 ±6.59^{abc}	79.75 ±7.19^{bc}	96.04 ±5.53^{ab}	72.15 ±8.41^{cd}	59.72 ±18.95^{de}
48 h	99.69 ±0.34^{a}	80.37 ±21.12^{bc}	74.66 ±6.14^{c}	6.25 ±17.68^{e}	91.52 ±4.66^{ab}	55.49 ±6.55^{d}	8.04 ±17.68^{e}	92.21 ±1.04^{ab}	79.58 ±5.46^{bc}	58.00 ±5.48^{d}
72 h	98.78 ±3.32^{a}	82.88 ±3.18^{b}	40.68 ±5.44^{d}	10.97 ±13.06^{e}	60.35 ±10.24^{c}	53.67 ±8.05^{cd}	8.75 ±18.08^{e}	87.08 ±2.8^{ab}	68.46 ±12.81^{c}	20.46 ±15.43^{e}
PC3 Prostate cancer										
24 h	95.99 ±2.19^{a}	80.14 ±6.69^{bc}	77.25 ±8.28^{bc}	45.04 ±13.74^{e}	84.2 ±8.17^{ab}	72.06 ±15.85^{bcd}	69.01 ±14.28^{cd}	94.05 ±2.43^{a}	93.29 ±1.68^{a}	59.56 ±4.99^{d}
48 h	98.79 ±1.1^{a}	65.52 ±12.34^{c}	65.68 ±14.66^{c}	12.66 ±8.98^{e}	82.32 ±5.36^{b}	67.17 ±12.34^{c}	21.31 ±13.15^{d}	82.04 ±5.00^{b}	81.9 ±4.58^{b}	32.88 ±5.95^{d}
72 h	95.71 ±3.04^{a}	50.03 ±7.35^{d}	43.64 ±12.7^{d}	0±0^{e}	75.79 ±7.66^{bc}	68.76 ±11.21^{bc}	0±0^{e}	78.74 ±5.07^{b}	64.19 ±11.66^{c}	9.75 ±10.05^{e}
SH-SY5Y Neuroblastoma										
24 h	90.51 ±4.82^{ab}	95.99 ±2.42^{a}	77.25 ±4.42^{cd}	13.71 ±11.61^{f}	85.01 ±10.05^{abc}	71.18 ±8.23^{de}	10.22 ±8.72^{f}	84.09 ±7.91^{abc}	82.36 ±8.85^{bcd}	65.44 ±9.72^{e}
48 h	99.75 ±0.21^{a}	98.25 ±0.95^{a}	57.64 ±9.08^{c}	0±0^{d}	99.78 ±0.29^{a}	62.88 ±8.49^{c}	0±0^{d}	98.94 ±0.95^{a}	86.42 ±4.79^{b}	0±0^{d}
72 h	99.65 ±0.31^{a}	81.32 ±11.69^{b}	45.62 ±6.41^{d}	0±0^{e}	84.34 ±8.57^{b}	62.89 ±6.86^{c}	0±0^{e}	98.72 ±0.83^{a}	96.46 ±1.98^{a}	0±0^{e}
L929 Mouse fibroblast										
24 h	98.91 ±0.87^{a}	92.01 ±7.24^{abc}	87.29 ±5.21^{bcd}	74.89 ±7.19^{e}	87.23 ±8.12^{bcd}	86.16 ±8.79^{cd}	9.46 ±7.00^{f}	95.71 ±2.37^{abc}	97.35 ±0.91^{ab}	79.62 ±12.76^{de}
48 h	99.25 ±0.82^{a}	82.49 ±10.8^{b}	66.72 ±15.54^{c}	33.39 ±19.83^{d}	88.99 ±6.98^{ab}	82.93 ±6.16^{b}	0±0^{e}	92.39 ±3.00^{ab}	91.04 ±4.44^{ab}	36.22 ±10.86^{d}
72 h	99.5 ±0.55^{a}	79.7 ±14.98^{b}	54.14 ±21.89^{d}	0±0^{e}	71.14 ±6.76^{bc}	65.7 ±6.08^{bcd}	0±0^{e}	61.79 ±9.42^{cd}	59.46 ±7.28^{cd}	14.19 ±17.53^{e}

Table 4. Caspase 3/7 activity assay results for PC3 and L929 cells.

Cell viability (%)	PC-3 control	PC-3 treated with **9a**	L929 control	L929 treated with **9a**
Living cells	95.0	81.6	98.6	95.4
Apoptotic cells	0.9	2.4	0.2	2.4
Dead cells	4.1	16.0	1.1	2.2

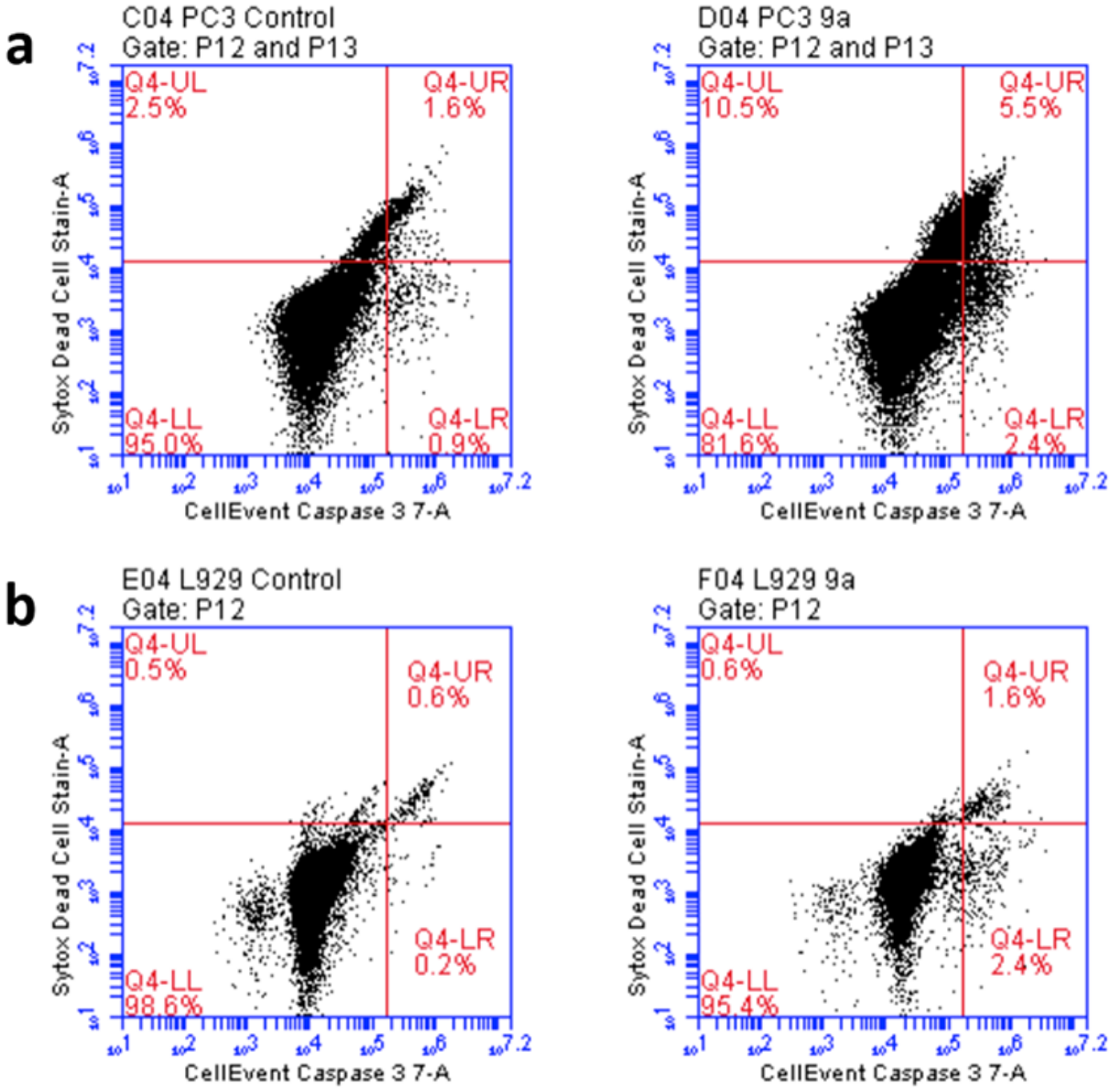

Figure 7. Caspase 3/7 activity assay results for a) PC3 and b) L929 cells. Lower left quadrants show the percentage of live cells while lower right quadrants show apoptotic cells. The sum of upper quadrants is the percentage of dead cells.

Methylene-tethered THQ structures were first synthesized in this work and **9a** had the lowest IC_{50} values for all cell lines. To answer the question arising from the effect of ring size on activity, we synthesized **11a** and **11b**, having five-membered rings fused to pyridine. **11a** and **9a** are structurally very similar and differ only in side chain size. When we evaluate our data, THQ **9a** was more toxic then the cyclopenta[*b*]pyridine **11a**. Saitoh et al. previously studied the relationship between structure and cytotoxicity of tetrahydroisoquinoline (TIQ) derivatives and bulky alkyl group-possessing TIQ structures showed more cytotoxicity against PC12 cells [36]. In another study, Ishihara et al. indicated that the higher toxicity of the TIQ moiety might be attributed to the molecular size rather than other physicochemical properties [37]. Our results also supported the importance of the function of molecular size on the cytotoxic behavior of THQs. These findings were consistent with the literature using different cancer cell lines. Hatano et al. also studied bulky substituents such as a 3,4-dimethoxybenzoyl group, an ethoxycarbonyl group, and a benzyloxycarbonyl group of TIQ moiety that showed the highest cytotoxicity and tumor-specificity to human squamous cell carcinoma cell lines (HSC-2, HSC-4) [35]. When cytotoxicity was evaluated in terms of concentration and time, compounds **9a**, **9b**, and **11a** at a low dose (50 µM) show little to no toxicity at 24 h and become toxic after 72 h. These findings may be attributed to the stability of moieties of THQ and cyclopenta[*b*]pyridine (except for the SH-SY5Y neuroblastoma cell line) in cell culture media. In fact, at 50 µM, compound **9a** allows SH-SY5Y cells to grow slightly faster as evidenced by viability values higher than 100 in Table 2. For the higher dose (300 µM), after 24 h compounds **9a** and **11a** showed rapid cytotoxic effects on the SH-SY5Y neuroblastoma cell line and compound **9b** on C6 cell line. After 72 h, at the higher dose (300 µM) compounds **9a**, **9b**, and **11a** were all cytotoxic to all cell lines.

Cytotoxicity was also evaluated by using AO/PI staining in terms of concentration and time, and compounds **9a**, **9b**, and **11a** at a low dose (50 µM) showed little to no toxicity at 24 h and became toxic after 72 h only for the PC3 cell line for compound **9a**, the MCF-7 cell line for compound **9b**, and the L929 cell line for compound **11b.** For the higher dose (300 µM), after 24 h, compounds **9a** and **9b** showed rapid cytotoxic effects on the SH-SY5Y neuroblastoma cell line and compound **11b** on the C6 cell line. After 72 h, at the higher dose (300 µM), compounds **9a**, **9b**, and **11a** were all cytotoxic to all cell lines. Cytotoxicity values showed differences, which might be due to the different interaction mechanisms of the MTT and AO/PI assays on the cells for the evaluation of cytotoxicity. As is well known, the MTT assay is based on the assumption that MTT tetrazolium salt reduction to formazan occurs in the mitochondria of living cells [38], whereas AO and PI are nucleic acid-selective stains and interact with DNA and RNA through intercalation or electrostatic attraction [31,32,39]. According to the Caspase 3/7 Activity Assay, compound **9a** induced more apoptosis of L929 cells than PC3 cells, whereas it induced necrosis of PC3 cells when compared to L929 cells. Both apoptotic and necrotic pathways were involved in the cell death of the PC3 and L929 cell lines after interaction with compound **9a** [40]. These findings may also be attributed to the stability and reactivity rate of the moieties of THQ and cyclopenta[*b*]pyridine in cell culture media. When all results were evaluated it was concluded that both methylene-tethered THQ and ketone moiety may have an influence on the cytotoxicity of cell lines in a concentration- and time-dependent manner. These results revealed that compound **9a** has a more suitable structure to be modified as a potential drug candidate.

Concerning the cell cytotoxicity studies, a swarming motility assay was performed using the gram-negative bacterium *Pseudomonas aeruginosa*, as swarming motility is one of three definite modes of motility observed in *P. aeruginosa*, characterized as movement across a semisolid surface [41,42]. According to the swarming motility assay, 1.5 mM **11a** showed 63% inhibition of swarming motility of the *P. aeruginosa* PA01 strain, while 1.5 mM

9a showed 74% inhibition (Figure 8). When these effects were compared to the control, the effects were found statistically significant (P <0.01). Compounds **11a** and **9a** are structurally very similar and differ only in side chain size; from these findings, we may conclude that even the ring size might affect the swarming motility of *P. aeruginosa*. With additional structural modifications and dose-dependent studies compound **9a** might be used as an inhibitor for the development of biofilms [43].

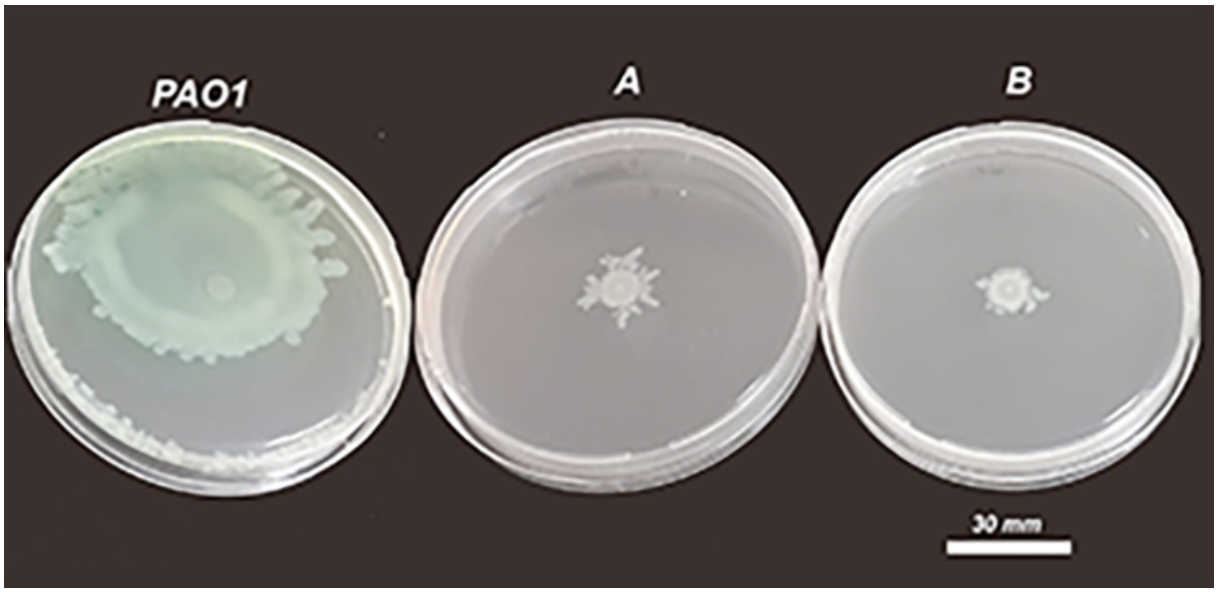

Figure 8. Swarming motility test for 1.5 mM concentration of compounds: a) compound **9a**, b) compound **11a**.

2.3. Conclusions

In this study, two different main skeletons were designed and synthesized starting from easily available materials under environmentally friendly conditions. Cytotoxic effects of all target structures were investigated on a panel of cancer cell lines of different tumors for rat glioblastoma (C6), human breast cancer (MCF-7), prostate cancer (PC3), neuroblastoma (SH-SY5Y), and mouse fibroblast (L929). Among them, **9a** induced the lowest IC_{50} values in all cell lines. The results indicated that the presence of the ketone moiety on **9a** enhanced the activity of the molecule towards all cells. **11a** exhibited lower cytotoxic activity than **9a**, and it is structurally very similar to **9a**, differing in the side chain size. SH-SY5Y showed fast cytotoxic response at 24 h to the higher dose (300 µM) of compounds **9a** and **11a**, as well as C6 cells for compound **9b**, which may lead to the conclusion that the stability of the **9a**, **9b**, and **11a** in cell culture media may change depending on cell type and time. Compound **9a** might be both involved in apoptotic and necrotic pathways in the cell death of the PC3 and L929 cell lines according to the Caspase 3/7 Activity Assay. When we take into account the AO/PI results, we may suggest that **9a** triggers more cell death mechanisms (apoptosis or necrosis) in PC3 cancer cells than L929 normal cells. Taking into account their cytotoxic effects on cancer cells, new methylene-tethered THQs and cyclopenta[*b*]pyridines are promising structures but need further structural modifications in order to enhance and/or change their cytotoxic properties to be considered as chemotherapeutic drugs. A swarming motility assay was performed with *P. aeruginosa* and compound **9a** showed higher inhibition of swarming motility, so it might be used as a possible biosurfactant and inhibitor for the formation of biofilms with additional studies.

3. Experimental

3.1. Materials and methods

All reagents were commercial and purchased from Acros Organics, Sigma-Aldrich, or Merck. ^{1}H NMR (400 MHz) and ^{13}C NMR (100 MHz) data were recorded on a Bruker DPX-400-ultra shield FT-NMR spectrometer in $CDCl_3$ with chemical shifts given in ppm relative to TMS as an internal standard. Melting points were determined with a Gallenkamp electrothermal digital melting point apparatus and are uncorrected. HRMS spectra were recorded on an Agilent (1200/6210) TOF LC/MS spectrometer. Reactions were monitored by TLC using precoated silica gel alumina plates (Kieselgel 60, F254, Merck) and visualized by UV lamp. Flash column chromatography was performed using silica gel (0.05–0.63 nm, 230–400 mesh ASTM, Merck).

3.1.1. Synthesis of Mannich base 7

2,6-Bis(morpholinomethyl)cyclohexanonedihydrochloride (**7**) was obtained from the reaction of cyclohexanone, paraformaldehyde, and morpholine hydrochloride according to the literature [1]. Pale yellow solid; yield: 57%; mp 163–164 °C. All spectral and physical data were in agreement with the published data.

3.1.2. Synthesis of Mannich base 10

2,5-Bis(morpholinomethyl)cyclopentanonedihydrochloride (**10**) was synthesized from the reaction of cyclopentanone, paraformaldehyde, and morpholine hydrochloride according to the literature [1]. White crystals; yield: 69%; mp 202–203 °C. All spectral and physical data were in agreement with the published data.

3.2. General procedure for synthesis of 9a and 9b

To a mixture of 2,6-bis(morpholinomethyl)cyclohexanonedihydrochloride (**7**) (0.20 g, 0.54 mmol), active methylene **8a** or **8b** (0.36 mmol), and ammonium acetate (0.16 g, 2.16 mmol) in 3 mL of water was added K-10 montmorillonite clay (0.36 g) and the mixture was heated at 80 °C for 1 h. After completion of the reaction (monitored by TLC), the reaction mixture was cooled to room temperature and 20 mL of water was added. The product was extracted with EtOAc (2 ×5 mL) and dried ($MgSO_4$). The solvent was removed under reduced pressure, and the residue was purified by flash column chromatography (silica gel, EtOAc/hexane, 1:6).

3.2.1. 1-(2-Methyl-8-methylene-5,6,7,8-tetrahydroquinolin-3-yl)ethanone (9a)

Pale yellow solid; yield: 64%; mp 64–65 °C; R_f = (0.6, EtOAc/hexane, 1:6); ^{1}H NMR (400 MHz, $CDCl_3$)δ: 7.69 (s, 1H), 6.37 (s, 1H), 5.20 (bs, 1H), 2.84 (t, J = 6.1 Hz, 2H), 2.72 (s, 3H), 2.65 (t, J = 6.1 Hz, 2H), 2.56 (s, 3H), 1.88 (p, J = 6.1 Hz, 2H); ^{13}C NMR (100 MHz, $CDCl_3$)δ: 200.0, 155.7, 153.5, 141.8, 138.3, 131.1, 129.0, 114.9, 32.2, 29.4, 29.2, 25.0, 22.8; ESI-HRMS (m/z): calcd. for $C_{13}H_{16}NO$ $[M+H]^+$: 202.1232; found: 202.1230.

3.2.2. Ethyl 2-methyl-8-methylene-5,6,7,8-tetrahydroquinoline-3-carboxylate (9b)

White crystals; yield: 52%; mp 41–42 °C; R_f = (0.7, EtOAc/hexane, 1:3); ^{1}H NMR (400 MHz, $CDCl_3$)δ: 7.91 (s, 1H), 6.36 (s, 1H), 5.19 (bs, 1H), 4.35 (q, J = 7.1 Hz, 2H), 2.82 (t, J = 6.1 Hz, 2H), 2.78 (s, 3H), 2.65 (t, J = 6.1 Hz, 3H), 1.86 (p, J = 6.1 Hz, 2H), 1.39 (t, J = 7.1 Hz, 3H); ^{13}C NMR (100 MHz, $CDCl_3$)δ: 166.7,

157.0, 153.8, 142.1, 139.5, 129.1, 123.9, 114.7, 61.0, 32.2, 29.3, 25.0, 22.8, 14.3; ESI-HRMS (m/z): calcd. for $C_{14}H_{18}NO_2$ $[M+H]^+$: 232.1338; found: 232.1345.

3.3. General procedure for synthesis of 11a, 11b, and 12

To a mixture of 2,5-bis(morpholinomethyl)cyclopentanonedihydrochloride (**10**) (0.20 g, 0.56 mmol), active methylene **8a** or **8b** (0.37 mmol), and ammonium acetate (0.17 g, 2.22 mmol) in 3 mL of water was added K-10 montmorillonite clay (0.37 g), and the mixture was heated at 80 °C for 1 h. After completion of the reaction (monitored by TLC), the reaction mixture was cooled to room temperature and 20 mL of water was added. The product was extracted with EtOAc (2 ×5 mL) and dried ($MgSO_4$). The solvent was removed under reduced pressure, and the residue was purified by flash column chromatography (silica gel, EtOAc/hexane, 1:6).

3.3.1. 1-(2-Methyl-7-methylene-6,7-dihydro-5H-cyclopenta[*b*]pyridin-3-yl)ethanone (11a)

Pale yellow solid; yield: 62%; mp 90–92 °C; R_f = (0.7, EtOAc/hexane, 1:3); ^{1}H NMR (400 MHz, $CDCl_3$)δ: 7.77 (s, 1H), 6.00 (bs, 1H), 5.18 (s, 1H), 2.93–2.89 (m, 2H), 2.84–2.80 (m, 2H), 2.68 (s, 3H), 2.51 (s, 3H); ^{13}C NMR (100 MHz, $CDCl_3$)δ: 200.4, 161.1, 157.7, 148.0, 136.7, 134.1, 131.7, 108.7, 29.5, 29.1, 27.1, 25.1; ESI-HRMS (m/z): calcd. for $C_{12}H_{14}NO$ $[M+H]^+$: 188.1075; found: 188.1084.

3.3.2. Ethyl 2-methyl-7-methylene-6,7-dihydro-5H-cyclopenta[*b*]pyridine-3-carboxylate (11b)

White crystal; yield: 50%; mp 58–59 °C; R_f = (0.6, EtOAc/hexane, 1:6); ^{1}H NMR (400 MHz, $CDCl_3$)δ: 8.07 (s, 1H), 6.08 (bs, 1H), 5.25 (s, 1H), 4.37 (q, J = 7.1 Hz, 2H), 2.95–2.90 (m, 2H), 2.90–2.85 (m, 2H), 2.83 (s, 3H), 1.40 (t, J = 7.1 Hz, 3H); ^{13}C NMR (100 MHz, $CDCl_3$)δ: 166.9, 161.5, 159.1, 148.1, 136.7, 135.5, 124.3, 108.6, 61.1, 29.1, 27.0, 25.0, 14.3; ESI-HRMS (m/z): calcd. for $C_{13}H_{16}NO_2$ $[M+H]^+$: 218.1181; found: 218.1176.

3.3.3. 1-(2,7-Dimethyl-6,7-dihydro-5H-cyclopenta[*b*]pyridin-3-yl)ethanone (12)

Yellow crystals; yield: 13%; mp 48–50 °C; R_f = (0.46, EtOAc/hexane, 1:3); ^{1}H NMR (400 MHz, $CDCl_3$)δ: 7.69 (s, 1H), 3.16–3.07 (m, 1H), 2.85–2.75 (m, 2H), 2.64 (s, 3H), 2.48 (s, 3H), 2.36–2.27 (m, 1H), 1.67–1.58 (m, 1H), 1.25 (d, J = 7.0, 3H); ^{13}C NMR (100 MHz, $CDCl_3$)δ:200.8, 171.0, 156.6, 133.6, 132.8, 130.6, 40.3, 32.4, 29.4, 28.4, 24.7, 18.7; ESI-HRMS (m/z): calcd. for $C_{12}H_{16}NO$ $[M+H]^+$: 190.1232; found: 190.1240.

3.4. In vitro cytotoxicity assay

Dulbecco's modified Eagle's medium supplemented with 10% FBS, 100 U/mL penicillin, and 100 µg/mL streptomycin was used to culture cells in a 5% CO_2 environment at 37 °C. Cells were seeded in 96-well plates (1×10^4 cells/well) 24 h prior to application of different **9a**, **9b**, and **11a** concentrations. After treatment with compounds **9a**, **9b**, and **11a** at concentrations 50, 100, and 300 µM, plates were incubated for 24, 48, and 72 h at 37 °C. Compounds **9a**, **9b**, and **11a** were dissolved in pure dimethyl sulfoxide (DMSO) to prepare stock solutions and diluted in complete growth medium to appropriate concentrations while keeping the final DMSO concentration below 1%. Stock solutions were stored at –20 °C.

Cytotoxicity of compounds **9a**, **9b**, and **11a** was determined with a commonly used procedure based on mitochondrial reductase activity of viable cells using MTT. Cells treated with compounds **9a**, **9b**, and **11a** were incubated in MTT reagent-containing medium for 3 h and water-insoluble dark blue formazan

crystals were solubilized in DMSO. The optical density of the dissolved material was measured at 570 nm (reference wavelength: 750 nm) using an automated microplate reader (Bio-Rad iMark). The mean IC_{50} is the concentration of compounds **9a**, **9b**, and **11a** that reduces cell viability by 50% under the experimental conditions and is the average of at least two independent, reproducible, and statistically significant measurements [44].

3.5. AO/PI staining

Each cell line was seeded in 48-well plates with a cell density of 104 cells/well. Drugs were applied at 50, 100, and 300 mM concentrations for 24-h, 48-h, and 72-h intervals. AO (5 mg/mL) and PI (3 mg/mL) stock solutions were prepared in ethanol and were diluted into PBS (1 µL/mL) prior to staining. At selected time points, cells were rinsed with PBS and 100 µL of staining solution was added to each well. Staining solutions were aspirated from wells after 1 min and cells were rinsed twice with PBS. Viable and nonviable cells were counted from 10 different areas for each experimental group using fluorescence microscopy [31,32].

3.6. Caspase 3/7 activity assay

PC3 and L929 cells were seeded into 6-well plates with a density of 1 million cells/well, and 24 h later, **9a** was administered at the IC50 values. After 72 h, growth media were aspirated from each well and kept aside. Cells were detached with 0.25% trypsin/EDTA solution and combined with their supernatants. Suspensions were centrifuged at 1000 rpm for 5 min and pellets were resuspended in 1 mL of growth medium. The CellEvent Caspase 3/7 Detection Kit was used to detect apoptosis. Caspase 3/7 detection reagent (1 µL) was added to each sample and incubated for 60 min at room temperature. Sytox AADvanced Dead Cell Stain Solution (1 µL) was added to each sample 5 min before the end of the incubation period. Measurements were taken with FL1 and FL3 lines of the flow cytometer (Accuri BD C6). At least 20,000 events were detected for each experimental group [34].

3.7. Swarming motility assay

Pseudomonas aeruginosa strain PAO1 was used for the evaluation of the swarming motility assay. For the assay, 100 µL of 1.5 mM **9a** and **11a** was added to 20 mL of medium, which contained 8 g/L nutrient broth, 5.0 g/L Bacto agar, and 0.5% glucose. After pouring the swarm medium, 5 µL each supernatant of the bacteria cultures was added to the middle of the medium. Plates were air-dried for about 15 min at room temperature and all plates were incubated overnight at 37 °C. The ability to swarm was assessed by the distance of swarming from the central inoculation site. Data were compared to PA01, which has ability to swarm [41,42].

3.8. Statistical analysis

Cytotoxicity results were expressed as mean ±SD. The data were analyzed using one-way ANOVA and significance was assigned at $P < 0.05$. IC_{50} values of substances were calculated by nonlinear regression analysis by homemade software, Helper of Cell Culture Lab.v.1 [44].

Acknowledgment

This work was partially supported by the Boğaziçi University Research Fund by Grant No. 6701.

References

1. Bray F, Ferlay J, Soerjomataram I, Siegel RL, Torre LA et al. Global Cancer Statistics 2018: GLOBOCAN estimates of incidence and mortality worldwide for 36 cancers in 185 countries. CA Cancer Journal for Clinicians 2018; 68 (6): 394-424. doi: 10.3322/caac.21492
2. Shankaraiah N, Jadala C, Nekkanti S, Senwar KR, Nagesh N et al. Design and synthesis of C3-tethered 1,2,3-triazolo-β-carboline derivatives: anticancer activity, DNA-binding ability, viscosity and molecular modeling studies. Bioorganic Chemistry 2016; 64 (2): 42-50. doi: 0.1016/j.bioorg.2015.11.005
3. Wan M, Xu L, Hua L, Li A, Li S et al. Synthesis and evaluation of novel isoxazolyl chalcones as potential anticancer agents. Bioorganic Chemistry 2014; 54 (6): 38-43. doi: 10.1016/j.bioorg.2014.03.004
4. Gedawy EM, Kassab AE, El-Malah AA. Synthesis and anticancer activity of novel tetrahydroquinoline and tetrahydropyrimidoquinoline derivatives. Medicinal Chemistry Research 2015; 24 (9): 3387-3397. doi: 10.1007/s00044-015-1388-7
5. Ghorab MM, Ragab FA, Heiba HI, Arafa RK, El-Hossary EM. Docking study, in vitro anticancer screening and radiosensitizing evaluation of some new fluorine-containing quinoline and pyrimidoquinoline derivatives bearing a sulfonamide moiety. Medicinal Chemistry Research 2011; 20 (3): 388-400. doi: 10.1007/s00044-010-9332-3
6. Rano T, Kuo GH. Improved asymmetric synthesis of 3,4-dihydro-2-[3-(1,1,2,2-tetrafluoroethoxy)phenyl]-5-[3-(trifluoromethoxy)phenyl]-alpha-(trifluoromethyl)-1(2H)-quinolineethanol, a potent cholesteryl ester transfer protein inhibitor. Organic Letters 2009; 11 (13): 2812-2815. doi: 10.1021/ol900639j
7. Rudenko DA, Shavrina TV, Shurov SN, Zykova SS. Synthesis and antioxidant activity of tricyclic compounds containing a 5,6,7,8-tetrahydroquinoline moiety. Pharmaceutical Chemistry Journal 2014; 48 (2): 100-103. doi: 10.1007/s11094-014-1057-z
8. Sridharan V, Suryavanshi PA, Menéndez JC. Advances in the chemistry of tetrahydroquinolines. Chemical Reviews 2011; 111 (11): 7157-7259. doi: 10.1021/cr100307m
9. Su DS, Lim JJ, Tinney E, Wan BL, Young MB et al. Substituted tetrahydroquinolines as potent allosteric inhibitors of reverse transcriptase and its key mutants. Bioorganic and Medicinal Chemistry Letters 2009; 19 (17): 5119-5123. doi: 10.1016/j.bmcl.2009.07.031
10. Gutiérrez M, Carmona U, Vallejos G, Astudillo L. Antifungal activity of tetrahydroquinolines against some phytopathogenic fungi. Zeitschrift für Naturforschung Section C Journal of Biosciences 2012; 67 (11): 551-556. doi: 10.5560/ZNC.2012.67c0551
11. Jo H, Choi M, Kumar AS, Jung Y, Kim S et al. Development of novel 1,2,3,4-tetrahydroquinoline scaffolds as potent NF-κB inhibitors and cytotoxic agents. ACS Medicinal Chemistry Letters 2016; 7 (4): 385-390. doi: 10.1021/acsmedchemlett.6b00004
12. Sabale PM, Patel P, Kaur P. 1,2,3,4-Tetrahydroquinoline derivatives and its significance in medicinal chemistry. Asian Journal of Research in Chemistry 2013; 6 (6): 599-610.
13. Roach SL, Higuchi RI, Adams ME, Liu Y, Karanewsky DS et al. Discovery of nonsteroidal glucocorticoid receptor ligands based on 6-indole-1,2,3,4-tetrahydroquinolines. Bioorganic and Medicinal Chemistry Letters 2008; 18 (12): 3504-3508. doi: 10.1016/j.bmcl.2008.05.029
14. Ogawa H, Yamashita H, Kondo K, Yamamura Y, Miyamoto H et al. Orally active, nonpeptide vasopressin V2 receptor antagonists:? a novel series of 1-[4-(benzoylamino)benzoyl]-2,3,4,5-tetrahydro-1H-benzazepines and related compounds. Journal of Medicinal Chemistry 1996; 39 (18): 3547-3555. doi: 10.1021/jm960133o
15. Wang XF, Wang SB, Ohkoshi E, Wang LT, Hamel E et al. N-Aryl-6-methoxy-1,2,3,4-tetrahydroquinolines: a novel class of antitumor agents targeting the colchicine site on tubulin. European Journal of Medicinal Chemistry 2013; 67 (1): 196-207. doi: 10.1016/j.ejmech.2013.06.041

16. Abd El-Salam OI, Abou El Ella DA, Ismail NSM, Abdullah M. Synthesis, docking studies and anti-inflammatory activity of some 2-amino-5,6,7,8-tetrahydroquinoline-3-carbonitriles and related compounds. Pharmazie 2009; 64 (3): 147-155. doi: 10.1691/ph.2009.8703

17. Calhoun W, Carlson RP, Crossley R, Datko LJ, Dietrich S et al. Synthesis and antiinflammatory activity of certain 5,6,7,8-tetrahydroquinolines and related compounds. Journal of Medicinal Chemistry 1995; 38 (9): 1473-1481. doi: 10.1021/jm00009a008

18. Yu GM, Mardanova LG, Kolla VE, Konshin ME. Synthesis, antiinflammtory and analgesic activities of 2-arylamino-5,6,7,8-tetrahydroquinoline-3-carboxamides. Pharmaceutical Chemistry Journal 1988; 22 (7): 554-556. doi: 10.1007/BF00763528

19. Zhang C, Hou T, Feng Z, Li Y. Structure-based development of antagonists for chemokine receptor CXCR4. Current Computer-Aided Drug Design 2012; 9 (1): 60-75. doi: 10.1126/science.1194396

20. Ghorab MM, Ragab FA, Hamed MM. Design, synthesis and anticancer evaluation of novel tetrahydroquinoline derivatives containing sulfonamide moiety. European Journal of Medicinal Chemistry 2009; 44 (10): 4211-4217. doi: 10.1016/j.ejmech.2009.05.017

21. Jirgensons A, Parsons C, Graham R, Jounzeme I, Kalvinsh I et al. Preparation of tetrahydroquinolinones and their use as antagonistts of Danysz Metabotropic glutamate receptors. Us Patent. US20050197361A1, 2005.

22. Faidallah HM, Saqer AA, Alamry KA, Khan KA, Asiri AM. Synthesis and biological evaluation of some novel tetrahydroquinolines as anticancer and antimicrobial agents. Journal of Enzyme Inhibition and Medicinal Chemistry 2014; 29 (3): 367-378. doi: 10.3109/14756366.2013.787421

23. Beattie DE, Crossley R, Curran AC, Dixon GT, Hill DG et al. 5,6,7,8-Tetrahydroquinolines. 4. Antiulcer and antisecretory activity of 5,6,7,8-tetrahydroquinolinenitriles and -thioamides. Journal of Medicinal Chemistry 1977; 20 (5): 714-718. doi: 10.1021/jm00215a019

24. Curran ACW, Crossley R, Hill DG. 8-amino-5,6,7,8-tetrahydroquinoline derivatives. US Patent 4011229 A, 1977.

25. Smith HW. Use of 5,6,7,8-tetrahydroquinolines and 5,6-dihydropyrindines as leukotriene and lipoxygenase inhibitors and the novel 3-substituted compounds therein. US Patent 4576949 A, 1984.

26. Smith HW. 5,6,7,8-Tetrahydroquinolines and 5,6-dihydropyrindines and their therapeutic use. Patent EP 0161867 A2, 1985.

27. Hanashalshahaby EHA, Unaleroglu C. Mannich bases as enone precursors for water-mediated efficient synthesis of 2,3,6-trisubstituted pyridines and 5,6,7,8-tetrahydroquinolines. ACS Combinatorial Science 2015; 17 (6): 374-380. doi: 10.1021/acscombsci.5b00046

28. Mauli R, Ringold HJ, Djerassi C. Steroids. CXLV.1 2-Methylandrostane derivatives. Demonstration of boat form in the bromination of 2α-methyl-androstan-17β-ol-3-one. Journal of American Chemistry Society 1960; 82 (20): 5494-5500. doi: 10.1021/ja01505a045

29. Roth HJ, Schwenke C, Dvorak G. Acetolyse des 2-Piperidinomethyl-cyclopentanons. 6. Mitt.: Acetolyse von Mannich-Basen. Archiv der Pharmazie (Weinheim) 1965; 298 (5): 326-335. doi: 10.1002/ardp.19652980510

30. Blicke FF, McCarty FJ. Disubstitution of cycloalkanones in the Mannich reaction. Journal of Organic Chemistry 1959; 24 (8): 1069-1076. doi: 10.1021/jo01090a009

31. Garipcan B, Odabas S, Demirel G, Burger J, Nonnenmann SS et al. In vitro biocompatibility of n-type and undoped silicon nanowires. Advanced Engineering Materials 2011; 13 (2): 3-9. doi: 10.1002/adem.200980045

32. Fani S, Kamalidehghan B, Lo KM, Hashim NM, Chow KM et al. Synthesis, structural characterization, and anticancer activity of a monobenzyltin compound against MCF-7 breast cancer cells. Drug Design, Development and Therapy 2015; 9: 6191-6201. doi: 10.2147/DDDT.S87064

33. Huang TC, Lee JF, Chen JY. Pardaxin, an antimicrobial peptide, triggers caspase-dependent and ROS-mediated apoptosis in HT-1080 cells. Marine Drugs 2011; 9 (10): 1995-2009. doi: 10.3390/md9101995

34. Breu A, Rosenmeier K, Kujat R, Angele P, Zink W. The cytotoxicity of bupivacaine, ropivacaine, and mepivacaine on human chondrocytes and cartilage. Anesthesia and Analgesia 2013; 117 (2): 514-522. doi: 10.1213/ANE.0b013e31829481ed

35. Hatano H, Takekawa F, Hashimoto K, Ishihara M, Kawase M et al. Tumor-specific cytotoxic activity of 1,2,3,4-tetrahydroisoquinoline derivatives against human oral squamous cell carcinoma cell lines. Anticancer Research 2009; 29 (8): 3079-3086.

36. Saitoh T, Abe K, Ishikawa M, Nakatani M, Shimazu S et al. Synthesis and in vitro cytotoxicity of 1,2,3,4-tetrahydroisoquinoline derivatives. European Journal of Medicinal Chemistry 2006; 41 (2): 241-252. doi: 10.1016/j.ejmech.2005.11.003

37. Ishihara M, Hatano H, Kawase M, Sakagami H. Estimation of relationship between the structure of 1,2,3,4-tetrahydroisoquinoline derivatives determined by a semiempirical molecular-orbital method and their cytotoxicity. Anticancer Research 2009; 29 (6): 2265-2271.

38. Śliwka L, Wiktorska K, Suchocki P, Milczarek M, Mielczarek S et al. The comparison of MTT and CVS assays for the assessment of anticancer agent interactions. PLoS One 2016; 11 (5): e0155772. doi: 10.1371/journal.pone.0155772

39. Varghese AC, Fischer-Hammadeh C, Hammadeh ME. Acridine orange test for assessment of human sperm DNA integrity. In: Zini A, Agarwal A (editors). Sperm Chromatin: Biological and Clinical Applications in Male Infertility and Assisted Reproduction. New York, NY, USA: Springer, 2011, pp. 189-199.

40. Yang J, Yang S, Zhou S, Lu D, Ji L et al. Synthesis, anti-cancer evaluation of benzenesulfonamide derivatives as potent tubulin-targeting agents. European Journal of Medicinal Chemistry 2016 122 (10): 488-496. doi: 10.1016/j.ejmech.2016.07.002

41. Rashid MH, Kornberg A. Inorganic polyphosphate is needed for swimming, swarming, and twitching motilities of *Pseudomonas aeruginosa*. Proceedings of the National Academy of Science of the USA 2000; 97 (9): 4885-4890. doi: 10.1073/pnas.060030097

42. Ha DG, Kuchma SL, O'Toole GA. Plate-based assay for swarming motility in *Pseudomonas aeruginosa*. Methods in Molecular Biology 2014; 1149: 67-72. doi: 10.1007/978-1-4939-0473-0_7

43. Hossain MA, Lee SJ, Park NH, Mechesso AF, Birhanu BT et al. Impact of phenolic compounds in the acyl homoserine lactone-mediated quorum sensing regulatory pathways. Scientific Reports 2017; 7 (1): 1-16. doi: 10.1038/s41598-017-10997-5

44. Rosselli S, Bruno M, Raimondo FM, Spadaro V, Varol M et al. Cytotoxic effect of eudesmanolides isolated from flowers of *Tanacetum vulgare* ssp. *siculum*. Molecules 2012; 17 (7): 8186-8195. doi: 10.3390/molecules17078186